AJNR Am J Neuroradiol 25:1544–1548, October 2004

Case Report

An Unusual Cause of Visual Loss: Involvement of Bilateral Lateral Geniculate Bodies

Pierre R. Lefèbvre, Monique Cordonnier, Danielle Balériaux, and Didier Chamart

Summary: We report the clinical and radiologic features of a 31-year-old woman who suffered incongruous binasal and bitemporal visual field defects and severe sudden visual loss due to hypoperfusion of bilateral lateral geniculate bodies following anaphylactic shock induced by 500 mg amoxicillin per os. Complete neuroophthalmologic examinations were performed regularly for visual acuity, color vision, pupillary reflexes, and visual fields. Additional testing was performed by means of MR imaging of the brain and CSF analysis. Follow-up was performed for 12 months. Vision loss was acute and severe, its onset bilateral and simultaneous. The patient recovered visual acuity of 1.0 within 7 weeks. Color vision was abnormal in both eyes but gradually improved to normal. Visual fields were characterized by incongruous binasal and bitemporal defects, but they reduced progressively. Cerebral MR imaging confirmed the presence of symmetrical lesions confined exclusively within both lateral geniculate bodies. These lesions were best seen on T1-weighted and fluid-attenuated inversion recovery images as high-signal-intensity areas suggestive of hemorrhagic ischemia. CSF analysis was normal and aseptic. Blood tests and cultures excluded any microbial infection. We conclude that shock may induce a bilateral isolated ischemia of the lateral geniculate bodies, resulting in incongruous binasal and bitemporal visual field defects and severe visual loss. MR imaging is the optimal imaging technique to confirm the diagnosis and for follow-up.

Bilateral involvement of the lateral geniculate bodies as a cause of visual disturbance is seldom reported in the literature. A report in 1933 by Mackenzie et al (1) describing lesions due to bilateral anterior choroidal syphilitic arteritis was followed in 1972 by a report by Merren (2), who described lesions arising due to bilateral coagulative necrosis thought to be induced by methanol toxicity. In 1995, Donahue et al (3) reported lesions arising due to geniculate myelinolysis, which was thought to be associated with the rapid correction of a hyponatremia, and in 1996 Greenfield et al (4) described lesions coexisting with a febrile gastroenteritis. The most recent report, in 2002, by Moseman and Shelton (5) reports geniculate lesions appearing in a preeclamptic woman the day after a caesarean delivery. In most of these cases, visual acuity was reduced, sometimes to light perception only, whereas visual fields exhibited mild to severe incongruous or congruous binasal and bitemporal defects. In the study by Moseman and Shelton (5), MR imaging revealed within the lateral geniculate bodies areas of symmetric bilateral decreased signal intensity on T1-weighted imaging (T1WI) and high-signal-intensity areas on fluid-attenuated inversion recovery (FLAIR) images and T2-weighted images (T2WI). These areas were consistent with acute infarcts. Greenfield et al (4) similarly described minimally increased signal intensity of both lateral geniculate bodies on T2WI, whereas Donahue et al (3) reported bilateral high-signal-intensity lesions in the lateral geniculate bodies on T2WI.

We report the clinical and radiologic features of a patient who suffered sudden incongruous binasal and bitemporal visual field defects and severe loss of vision following anaphylactic shock.

Received December 18, 2003; accepted after revision February 14, 2004.

From the Departments of Ophthalmology (P.R.L., M.C.) and Neuroradiology (D.B.), Hôpital Erasme, Université Libre de Bruxelles, Brussels, Belgium; and the Department of Internal Medicine, Institut Médico-Chirurgical d'Ath (D.C.), Ath, Belgium.

Address correspondence to Pierre R. Lefèbvre, MD, Department of Ophthalmology, Hôpital Erasme, 808 route de Lennik, B—1070 Brussels, Belgium.

Case Report

The patient is a 31-year-old woman who self-prescribed amoxicillin for a throat infection. Immediately after swallowing the drug, the patient began to feel her face swell and collapsed. She was taken to the emergency ward, where additional reactions, including Quincke angioneurotic edema, a truncular papulomacular rash, and major hypotension, were noted. These reactions were resolved by intravenous adrenaline and methylprednisolone. The following day, the patient complained of visual disturbances. A complete ophthalmologic examination was performed, comprising tests for visual acuity, color vision (Ishihara testing), pupillary reflexes, intraocular pressure, and visual fields. Examination of the anterior and posterior segments was also performed.

Further testing was carried out, including electroencephalogram (EEG), MR imaging of the brain, and CSF analysis. Standard blood tests were performed. The possibility of microbial involvement was tested by means of serology and by blood, CSF, throat, and urinary cultures. Corticosteroid therapy was given only to treat the anaphylactic shock. No further treatment was administered.

Ophthalmologic follow-up, including visual acuity, color vision (Ishihara testing), pupillary reflexes, and visual field testing, were performed regularly over the course of the following 12 months. Follow-up MR imaging was performed at 6, 16, and 51 days and 12 months after the initial onset of symptoms. Severe loss of vision was noticed the day after treatment for the anaphylactic shock.

First Examination

The best-corrected visual acuity on Snellen chart was 20/100 in each eye. Compared with someone with no visual acuity impairment—having 20/20 vision on the Snellen chart—an

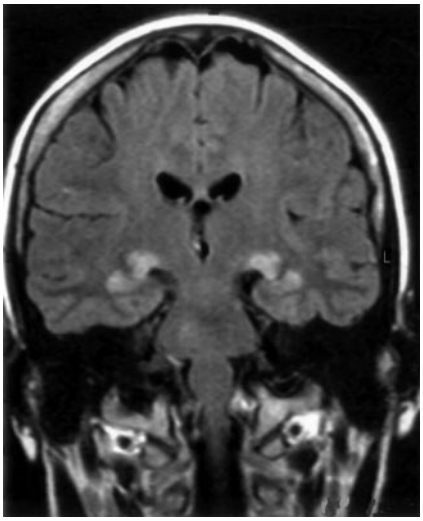

FIG 1. Coronal FLAIR image obtained 1 day after the acute onset of anaphylactic shock symptoms, showing bilateral hyperintense areas symmetrically located within the lateral geniculate bodies and extending laterally within the white matter of the parahippocampal regions.

image 20 feet away had to be enlarged five times to be recognized by a person with 20/100 visual acuity. Bilateral, severe color vision abnormalities were demonstrated. Photomotor reflex was present in both eyes, and there was no evidence of relative afferent pupillary defect. Visual field testing revealed macular splitting and incongruous binasal and bitemporal visual field defects; the foveal thresholds were clearly reduced, which indicates that the foveae could see only spots of high luminous intensity. Intraocular pressure, slit lamp examination, and fundi were otherwise normal.

Initial MR imaging of the brain was performed 1 day after the acute onset of shock symptoms. During this examination, bilateral hyperintense areas symmetrically located within the geniculate bodies and extending laterally within the white matter of the parahippocampal regions were best demonstrated on coronal FLAIR images (Fig 1). T1WI findings at this time were normal, and no contrast enhancement was seen after gadolinium (Gd) injection.

A second MR examination, performed 5 days later, again revealed hyperintense lesions on FLAIR images. On this occasion, however, intense enhancement at the level of both geniculate bodies and extending to the superior parahippocampal regions was observed on T1WI after Gd administration (Fig 2).

The neurologic examination and EEG findings were both normal. CSF analysis revealed a protein level of 44 mg/dL (normal range, 20–45 mg/dL), a glucose level of 67 mg/dL (normal range, 50–80 mg/dL), and a white blood cell count of 1/mm^3 (normal level, < 6/mm^3). The CSF culture, as well as the throat smear and the blood and urine cultures, were negative.

Serologic tests, including the Venereal Disease Research Laboratory, Treponema pallidum hemagglutination, Paul Bunnel-Davidsohn test, anti-Epstein Barr–virus M-immunoglobulins, surface B-hepatitis antigen, and C-hepatitis antibodies, were all negative. The anti-Epstein Barr–virus G-immunoglobulins, however, were >170 arbitrary units/mL.

The erythrocyte sedimentation rate was 18 mm/h. C-reactive protein was measured at 7.2 mg/dL on admission, but was reduced to 1.2 mg/dL 4 days later. Similarly, the white blood cells count was 12,600/mmł at admission and 9500/mmł 4 days later. Ionogram was normal, except for a hypokaliemia at 2.8 mEq/L that was resolved the day after. No toxin screen was performed (no anamnestic clues for toxic use).

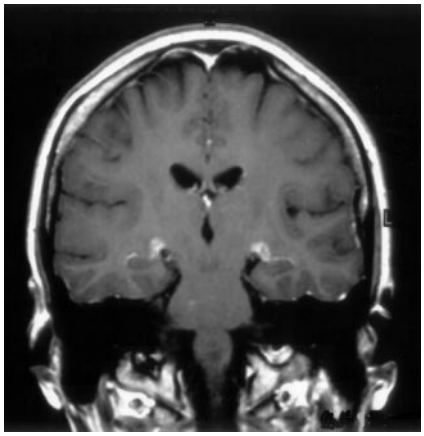

FIG 2. Coronal Gd-enhanced T1WI obtained at day 6. Enhancement within both geniculate bodies extending to the superior parahippocampal regions is clearly visible.

Follow-up

The patient was followed and examined periodically in the 12 months after onset. No treatment was prescribed during this time, except for cetirizine (antihistaminic-1) for 3 weeks. The patient recovered a stable best-corrected visual acuity of 20/20 on the Snellen chart after 7 weeks. Color vision normalized within 3 months. Visual field defects, including involvement of macular bundles, were reduced, while at 12 months temporal defects and severe binasal involvement had set in. The foveal threshold, however, had improved in both eyes to subnormal, which indicates that spots of low luminous intensity could again be noticed. Optic disks at 12 months exhibited temporal pallor.

Follow-up MR imaging was performed 16 days after the acute onset. On sagittal and coronal T1WI, the geniculate bodies appeared hyperintense before contrast medium injection (Fig 3A). On axial and coronal FLAIR images, the lesions were still visible, although the extent and intensity of the abnormal high signal intensity were decreased (Fig 3B). Mild contrast medium uptake was still evident on T1WI after Gd injection (Fig 3C). Finally, on gradient echo T2WI, small hypointense areas were evident, which were consistent with hemosiderin deposits. This confirmed the hemorrhagic component of these presumably ischemic lesions (Fig 4). Diffusion-weighted images were normal.

An additional MR imaging examination was performed at 51 days after acute onset. On T1WI, the lesions were very discreetly hyperintense (Fig 5A), whereas normal findings were seen on FLAIR images (Fig 5C). Iron deposits were still clearly visible on gradient echo T2WI, whereas mild but persistent contrast uptake was still apparent on T1WI after Gd injection (Fig 5*C*).

A final MR imaging examination comprising T1WI, T2WI, FLAIR, gradient echo T2WI, and Gd-enhanced T1WI was performed at 12 months. The iron deposits, seen as small hemorrhagic residual lesions, were still visible on gradient echo T2WI. All images obtained with the other pulse sequences were strictly normal.

Discussion

The dorsal nucleus of a lateral geniculate body is the relay station for the axons from the retinal ganglion cells (6). Its vascular supply (6, 7) derives from both the anterior choroidal artery for the anterolateral part of the nucleus and the hilum and the lateral posterior choroidal artery for the rest of the nucleus and the hilum of the lateral geniculate body. These

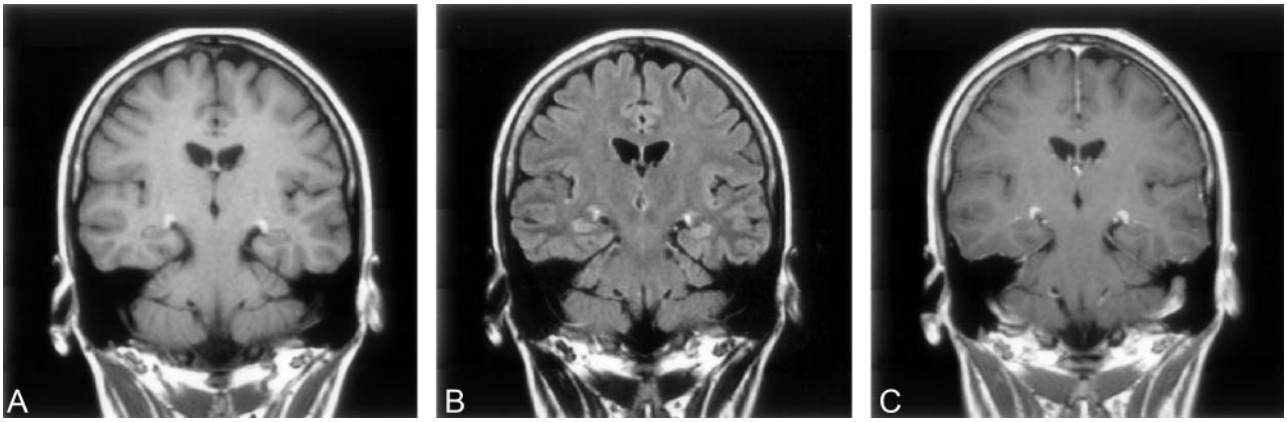

FIG 3. Control MR images obtained 16 days after onset of symptoms.
A, Coronal T1WI, in which the geniculate bodies appear hyperintense.
B, Coronal FLAIR image, in which lesions are still visible but the extent and intensity of the abnormal high signal intensity are decreased.
C, Coronal Gd-enhanced T1WI, in which mild contrast uptake is still evident.

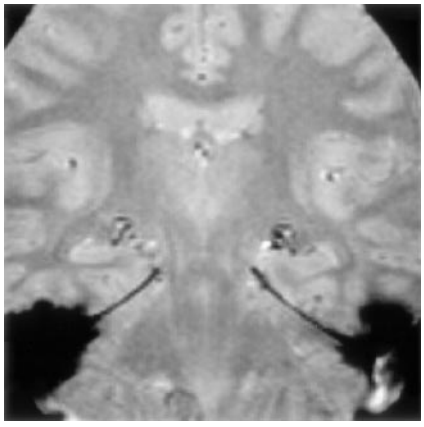

FIG 4. Coronal gradient echo T2WI obtained at day 16, demonstrating small hypointense areas in both geniculate bodies corresponding to hemosiderin deposits.

two networks are anastomotic in the intervening region of the lateral geniculate body, which includes the hilum, but are thin and terminal.

Visual field abnormalities complicate the one-sided occlusion of the anterior or lateral posterior choroidal artery as devised by Luco et al (8). Because of the retinotopy within the lateral geniculate bodies (9), occlusion of the anterior choroidal artery produces a superior or inferior homonymous sectoranopia, which leads to a hemihourglass-shaped visual field defect. Conversely, occlusion of the lateral posterior choroidal artery produces a horizontal wedge-shaped homonymous sectoranopia that similarly leads to a hemihourglass-shaped visual field (8, 10–13). Visual field defects associated with involvement of the unilateral lateral geniculate body tend to be most commonly incongruent except when associated with a vascular origin (8, 10, 11): even if the blood supply of the lateral geniculate body is dual and offers a theoretical protection against ischemia, a sudden arterial obstruction can lead to necrosis before the effectiveness of the anastomotic network (2) and therefore to congruent visual field defects. This vascular-induced congruency of visual field lesions is, however, not always seen because of the anastomotic network of the lateral geniculate body in its intervening region. Two more factors may be related to the incongruency of the visual field defects despite a vascular origin: the amount of interpersonal variability in the structure of the human lateral geniculate body, well described by anatomic studies by Hickey and Guillery (6, 14), so the one-sided artery does not supply the same territory in everybody, and the fact that branches originating from the posterior communicating artery may feed the territory supplied by the anterior choroidal artery (7).

In our patient, both lateral geniculate bodies were involved, and an infectious etiology could reasonably be ruled out. Visual field defects were right- and left-homonymous incongruent (more pronounced in the nasal visual fields) and involved the macular region. Moreover, there was no obvious sectoral or wedge-shaped defect. This suggests a vascular origin that is bilateral and involves both the lateral posterior and anterior choroidal arteries. The evolutionary aspects of the MR images are consistent with the diagnosis of bilateral acute ischemic lesions that become slightly hemorrhagic. The pattern of contrast medium uptake is also in accordance with known evolutionary aspects of acute ischemia. Gradient echo images and nonenhanced T1WI clearly show the hemorrhagic transformation. Diffusion-weighted images were not helpful in this case, but this may have been due to the delay of acquisition (16 days after the onset of symptoms). At this point, the small size of the lesions may have limited their visibility on diffusion-weighted images. Shock-induced ischemia is the most likely cause for the involvement of both lateral geniculate bodies in this case. The hemorrhagic transformation seen on MR images may be related to ensuing blood brain–barrier disruption (15, 16) in the territory supplied by both the anterior and lateral posterior choroidal arteries. This leads to cellular dysfunction within the two lateral geniculate bodies and to the resulting visual symptoms.

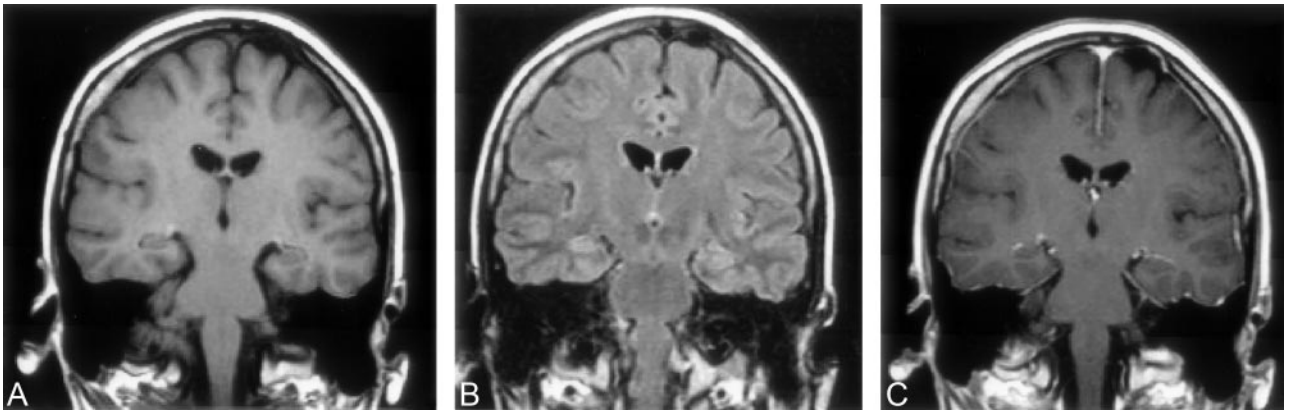

FIG 5. Follow-up MR images obtained at day 51.
A, Coronal T1WI, in which lesions are very discreetly hyperintense.
B, Normal FLAIR image.
C, Gd-enhanced T1WI, in which the lesions are still visible but are reduced in size and contrast uptake is mild.

The lateral geniculate bodies are a peculiar location for reactions following anaphylactic shock, which has, to the best of our knowledge, never been described before. These bodies are relatively close to the putamen and thus can be considered as a part of the border zone between the parietal, temporal, and occipital regions where the vascular network becomes thinnest and ends (17, 18). As described by Mull (19), these border zones between the anterior, medium, and posterior brain territories are watershed areas; they are most susceptible to critically decreased perfusion pressure and can lead to hemodynamic infarction. The most vulnerable location within the periventricular territory is usually the lenticulostriate nucleus. Underperfusion can damage the watershed areas, especially if associated with an incompetent circle of Willis. This is often demonstrated effectively by MR angiography. According to Macchi et al (20) and Krabbe-Hartkamp et al (21), a complete circle of Willis occurs in only 41% and 42% of people, respectively, and is more frequent in younger people (22). No reports mention an age-related development of collateral arteries. Severe hypotension occurring in the parietotemporooccipital areas can induce bilateral watershed infarction (23–25), whose most common features are cerebral blindness and visual disorientation (24).

The vascular architecture of the lateral geniculate bodies in this case probably led to their ischemia because of its anatomic structure and of the thinness of its terminal blood supply. MR angiography has not been achieved, because of the narrow diameter of these arteries, nor has selective arteriography because of the risks of this invasive procedure. They could, however, still be performed to reveal an incompetent circle of Willis, which might be associated with shock-induced underperfusion having led to the damage of both lateral geniculate bodies.

Conclusion

This case demonstrates that shock may induce isolated ischemia of both lateral geniculate bodies resulting in incongruous binasal and bitemporal visual field defects and severe loss of vision. MR imaging is the optimal imaging technique to confirm the diagnosis and for follow-up.

References

1. Mackenzie I, Meighan S, Pollock EN. **On the projection of the retinal quadrants on the lateral geniculate bodies, and the relationship of the quadrants to the optic radiations.** *Trans Ophthalmol Soc U K* 1933;53:142–169
2. Merren MD. **Bilateral lateral geniculate body necrosis as a cause of amblyopia.** *Neurology* 1972;22:263–268
3. Donahue SP, Kardon RH, Thompson HS. **Hourglass-shaped visual fields as a sign of bilateral lateral geniculate myelinolysis.** *Am J Ophthalmol* 1995;119:378–380
4. Greenfield DS, Siatkowski RM, Schatz NJ, Glaser JS. **Bilateral lateral geniculitis associated with severe diarrhea.** *Am J Ophthalmol* 1996;122:280–281
5. Moseman CP, Shelton S. **Permanent blindness as a complication of pregnancy induced hypertension.** *Obstet Gynecol* 2002;100:943–945
6. Miller NR. *Walsh & Hoyt's Clinical Neuro-ophthalmology.* Vol 1. 4th ed. Baltimore: Williams & Wilkins;1982:69–78
7. Kupersmith MJ, Berenstein A. *Neurovascular Neuro-ophthalmology.* Berlin, New York: Springer-Verlag; 1993: 40–42, 375–378
8. Luco C, Hoppe A, Schweitzer M, et al. **Visual field defects in vascular lesions of the lateral geniculate body.** *J Neurol Neurosurg Psychiatry* 1992;55:12–15
9. Shacklett DE, O'Connor PS, Dorwart RH, et al. **Congruous and incongruous sectorial visual field defects with lesions of the lateral geniculate nucleus.** *Am J Ophthalmol* 1984;98:283–290
10. Lee AG, Brazis PW. *Clinical Pathways in Neuro-ophthalmology: An Evidence-Based Approach.* New York: Thieme;1998:158–159
11. Vignal C, Miléa D. *Neuro-ophtalmologie.* Paris: Elsevier;2002:164–167
12. Frisen L, Holmegaard L, Rosencrantz M. **Sectorial optic atrophy and homonymous, horizontal sectoranopia: a lateral choroidal artery syndrome?** *J Neurol Neurosurg Psychiatry* 1978;41:374–380
13. Frisen L. **Quadruple sectoranopia and sectorial optic atrophy: a syndrome of the distal anterior choroidal artery.** *J Neurol Neurosurg Psychiatry* 1979;42:590–594
14. Hickey TL, Guillery RW. **Variability of laminar patterns in the human lateral geniculate nucleus.** *J Comp Neurol* 1979;183:221–246
15. Petty MA, Wettstein JG. **Elements of cerebral microvascular ischaemia.** *Brain Res Brain Res Rev* 2001;36:23–34
16. Mayer TE, Schulte-Altedorneburg G, Droste DW, Bruckmann H. **Serial CT and MRI of ischemic cerebral infarcts: frequency and clinical impact of hemorrhagic transformation.** *Neuroradiology* 2000;42:233–239
17. Salamon G. *Atlas of the arteries of the human brain.* Paris: Asclepios; 1973:160–161
18. Duvernoy HM. *Le cerveau humain: surface, coupes sériées et IRM.* Paris: Springer-Verlag;1992:135–136

19. Mull M. **Hemodynamically induced cerebral infarcts: clinical significance of infarct pattern and angiomorphology.** *Radiologe* 1997; 37:871–877
20. Macchi C, Catini C, Federico C, et al. **Magnetic resonance angiographic evaluation of circulus arteriosus cerebri (circle of Willis): a morphologic study in 100 human healthy subjects.** *Ital J Anat Embryol* 1996;101:115–123
21. Krabbe-Hartkamp MJ, van der Grond J, de Leeuw FE, et al. **Circle of Willis: morphologic variation on three-dimensional time-of-flight MR angiograms.** *Radiology* 1998;207:103–111
22. Guerin J, Gouaze A, Lazorthes G. **The circle of Willis in children and the factors shaping it.** *Neurochirurgie* 1976;22:217–226
23. Bogousslavsky J, Regli F. **Borderzone infarctions distal to internal carotid artery occlusion: prognostic implications.** *Ann Neurol* 1986; 20:346–350
24. Howard R, Trend P, Russell RW. **Clinical features of ischaemia in cerebral arterial border zones after periods of reduced cerebral blood flow.** *Arch Neurol* 1987;44:934–940
25. Franck G. **Border zone ("watershed area") cerebral ischaemia.** *Electroencephalogr Clin Neurophysiol Suppl* 1982;35:297–306